CHAPTER 3

RESULTS AND DISCUSSION FOR CADMIUM TELLURIDE (CdTe)

3. RESULTS AND DISCUSSION FOR CADMIUM TELLURIDE (CdTe)

The following chapter presents all the data and relevant discussions based on the material characterisation and electrical characterisation of the electrodeposited and sputtered films of CdTe and the variations applied to the preparation of them. The focus is largely on electrodeposition of CdTe on silicon wafers obtained as rejects from the wafer industry and subsequent formation as solar cells.

Not all silicon wafers are suitable for the manufacture of solar cells as there are properties such as resistivity and type which need to be considered. For the following chapters 3, 4 and 5, the silicon substrates that were used is shown in table 3.1 and are referred to by the subscribed type numbers:

Table 3.1 The type of wafers and associated properties

WAFER TYPE	RESISTIVITY	SIZE	TYPE
Type I	4.3 Ωcm	4"	n-type
Type II	16.96 Ωcm	4"	p-type
Type III	<0.1 Ωcm	5"	p-type
Type IV	1.806 Ωcm	5"	p-type
Type V	9.6 Ωcm	8"	p-type

Apart from the above mentioned silicon wafers, the samples will also be deposited on two grades of indium tin oxide (ITO) glass and on normal glass (sputtering only). The purpose of preparing these samples on a transparent substrate is so that the optical analysis can be done for characterisation purposes.

3.1 Analysis Procedure

The following section outlines the experimental approach and the procedure for coating the required thin films from the initial setting up stages until the final verification and characterisation measures. These procedures were repeated for all the experimental results and discussions chapters which are chapters 3, 4 and 5.

3.1.1 Sequence of Events

1. The first stages of the research involve obtaining the relevant chemicals and materials such as silicon wafers and ITO glass. Following this, an apparatus setup for electrodeposition was made and tested for functionality.

2. Following this, optimisation of all electrodeposition parameters as prescribed by prior research [49, 57, 64, 65] was done and the outcome carefully observed. Among the major parameters studied and tested were:

- Deposition voltage
- Deposition time
- Counter electrode material
- Temperature

3. When these parameters were corrected, the final preparation of samples were done and subjected to the following characterisation techniques:

- X-ray Diffraction - For phase analysis and verification
- Energy Dispersive Analysis of X-rays - Quantitative analysis
- Scanning Electron Microscopy - Study of surface morphology
- Ultra violet-Visible Spectroscopy - To obtain thickness, refractive index, absorption coefficient and energy gap

4. Finally, after the material had been properly characterised and identified, it was subjected to solar cell characterisation studies. The following studies were done :

- Open circuit voltage (OCV) and Short circuit current (I_{SC})
- Current - Voltage characteristics - To form the I-V characteristic curve

As discussed in earlier chapters, the basic intention of this research is to fabricate the ternary compound, **$CdTe_XSe_{1-X}$**, from two binary semiconducting compounds, CdTe and CdSe. This is predicted to have a favourable effect on the photovoltaic properties

due to alterations in the energy gap to better match that of the peak of the solar radiation spectra. In order for such a comparative assumption to be made, it is absolutely necessary to study the individual materials, which are CdTe and CdSe, individually first. In this chapter the results obtained from the analysis of CdTe is presented as per the guidelines described in the analysis procedure. Further, the $CdTe_XSe_{1-X}$ compounds were deposited on waste silicon wafers obtained from local industries.

3.2 Electrodeposition of CdTe

The electrodeposition is a fairly simple technique in the aspect of conducting the relevant experiments but requires a great deal of preparation and care in the setting up stage. After the apparatus has been set up as described in chapter 2 , the following parameters were taken into account.

3.2.1 The Electrolyte

The electrolyte provides the free ions of cadmium and tellurium to be mobile in the liquid phase and thus enables the deposition to take place on the electrode. In this circumstance, the electrode process that takes place is known as a cathodic deposition whereby the targeted material of CdTe forms on the negative electrode. Naturally for this phenomenon to take place the electrodes and electrolyte have to be conducting or at least semiconducting.

It is also important to consider the concentration of the salts as the deposition content can vary with concentration. As earlier described in chapter 2, it is important to first study the cathodic polarisation properties and the voltammograms from published matter [66]. From these journals it was found that the electroactive range for CdTe deposition in silicon is found by first studying its electrochemical behaviour.

The prescribed component chemicals necessary for the electrodeposition of CdTe are $CdSO_4$ and TeO_2. Alternately $CdCl_2$ can also be used in place of $CdSO_4$. In figure 3.1

the voltammogram for the component electrolytes and the combination for both are shown.

From the voltammogram, we can see that the cadmium deposition starts at -750mV and the large current intensity increase results from the large Cd^{2+} concentration of the solution (0.5M). On the other hand, the concentration used for the tellurium solution is low (5mM) and a first wave at -400mV can be attributed to $HTeO_2^+$ reduction, leading to a Te deposit. A second wave occurs at -700mV which may be attributed to the tellurium reduction into H_2Te (aq).

Fig 3.1 also shows the voltammogram obtained from the electrolyte containing both species in solution. The reduction of $HTeO_2^+$ still occurs at -400mV, and between -400mV and -700mV, there is codeposition of CdTe. The reduction of Cd^{2+} above its redox potential is made possible due to the gain in free energy upon alloy formation, $\Delta G = -99 kJmol^{-1}$. The global reaction mechanism is:-

$$Cd^{2+} + HTeO_2^+ + 3H^+ + 6e^- \rightarrow CdTe + 2H_2O$$

The large increase in current at the end of the plateau (above -760mV) is due to the electrodeposition of metallic cadmium.

Care has to be taken not to place the silicon electrodes in the electrolyte solution for too long as a brown coating of tellurium can be formed under open circuit conditions via a corrosion mechanism which can be explained by the coupled redox reactions:

Oxidation mechanism : $Si + 2H_2O \rightarrow SiO_2 + 4H^+ + 4e^-$

Reduction mechanism : $HTeO_2^+ + 4e^- \rightarrow Te + 2H_2O$

This process then results in the oxidation of the surface silicon atoms. In order to minimise electroless deposition of elemental tellurium, the potential was stepped to the required deposition potential immediately after immersion of the sample.

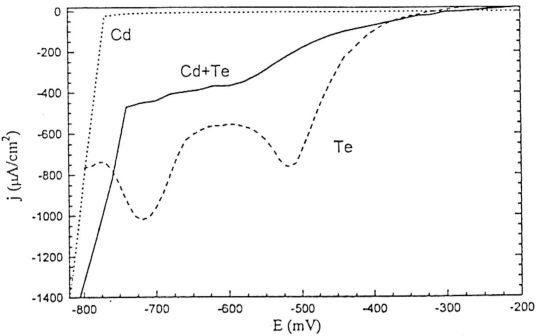

Figure 3.1 : Voltammogram for Cadmium (0.3M), Tellurium (1mM) and CdTe (Combined)

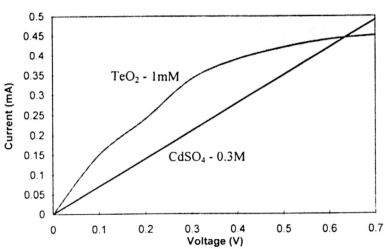

Figure 3.2 : Cathodic Polarisation Curve for Cadmium (0.3M) and Tellurium (1mM)

Another method of obtaining the deposition potential is by investigating the cathodic polarisation characteristics as described in chapter 2. The cathodic polarisation curve is shown in figure 3.2. Supported by the voltammogram, it is possible to narrow down the potential down to a more practical value. Films of CdTe have been accurately coated [49, 64, 65] by utilising a voltage between 500mV and 750mV, dependant on substrate type and bath concentration.

In this research, similar voltage variation was applied to an electrolyte containing the following analar grade chemicals:

1. $CdSO_4$ - 0.3M
   OR
   $CdCl_2$ - 0.3M
2. TeO_2 - 1mM
3. Ethylene-diamine-tetra acetic acid (EDTA) - 15mM

Since the solubility of TeO_2 is extremely low, it has to be first dissolved in concentrated acid before water is added. Hydrochloric acid is used in conjunction with $CdCl_2$ and sulphuric acid is used with $CdSO_4$. The purpose of EDTA is to function as a complexing agent which forms a complex with the impurities that comes with the salt, if any, and to increase the overall conductivity. The presence of the acid (sulphuric or hydrochloric) ensures that the electrolyte is always in an acidic media. For the purpose of comparison, the deposition was repeated with and without EDTA and the difference observed.

3.2.2 The Electrodes

A variety of working electrodes (cathodes) were used for the electrodeposition purpose. For the fabrication of solar cells, five grades of silicon wafers were used as well as two grades of ITO glass. The silicon wafers were cut into rectangles measuring about 2cm x 3cm and put through the cleaning process prescribed in chapter 2. When ITO glass was used, it was cleaned in a detergent solution and rinsed in distilled water before being cleaned in an ultrasonic cleaner repeatedly with detergent and distilled water.

Finally it was washed and rinsed with acetone to remove all traces of grease from the surface.

During the initial stages, the deposition on silicon type V was experimented with a variety of counter electrodes such as platinum, copper and silicon. Of all these counter electrodes, copper yielded the highest deposition current at 0.67V and deemed the most suitable for this purpose. The table below outlines the electrode type and the respective deposition current.

Table 3.1 Deposition current for various counter electrodes

Counter electrode (Anode)	Current (mA)	Voltage (V)
Pt	0.01	0.67
Cu	1.5	0.67
Si	0.1	0.67

When platinum and silicon were used as counter electrodes, there was no visible film formed even though the deposition was left to take place for 24 hours. Consequently, all the deposition was done using copper as the counter electrode.

However, caution has to be taken when copper is used as Cu^{2+} ions are inclined to diffuse into the electrolyte and subsequently onto the samples in prolonged periods of time [67]. Figure 3.3a and figure 3.3b show the EDX spectra of an electrodeposition of n-CdSe onto p-Si for a period of thirty minutes and three hours respectively at a deposition voltage of 0.67V. After the deposition had taken place, the coating on silicon was rinsed with distilled water and left to dry.

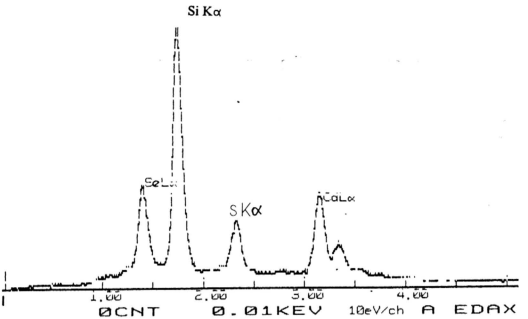

Figure 3.3a : EDX Spectra for CdSe Electrodeposited on Si at 0.7V for 30 minutes

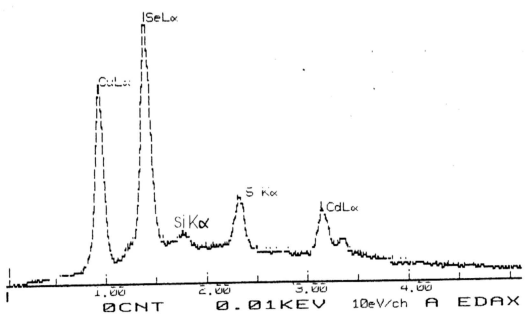

Figure 3.3b : EDX Spectra for CdSe Electrodeposited on Si at 0.7V for 120 minutes

From figure 3.3a, we can see that the CdSe is very thin as the electron beam can easily penetrate through the CdSe layer and in turn excite silicon atoms of the substrates to obtain a high fluorescence yield and thus a silicon high peak. The deposition ratio of cadmium and selenium is approximately 1:1 forming a good thin coating of CdSe which is suitable for solar cell applications.

In figure 3.3b, where the electrodeposition was allowed to take place for three hours, it can be observed that a thick film was formed as the silicon peaks were subdued. Most prominent was the fact that copper had diffused into the coating as observed with the CuLα peak. This long deposition rate has also caused a shift in the composition whereby the concentration of selenium has shifted dramatically with respect to cadmium. This could be explained by the exhaustion of Cd ions. It was also noted that the electrolyte had changed colour from clear to light blue. Presumably, the Cu^{2+} ions had combined with free SO_4^{2-} ions to form $CuSO_4$, explaining the blue coloured solution.

Another precautionary measure taken was to change the copper counter electrode at five minutes interval during the electrodeposition process. This was done as the copper electrode tends to oxidise rapidly in the presence of acids in the electrolyte.

The presence of sulphur (SKα) in both the EDX spectra is undesirable as it can form a complex compound with copper and selenium to give rise to an unpredicted compound. Therefore, ensuing electrolytes were made also with $CdCl_2$ instead of $CdSO_4$ (origin of sulphur) and the difference compared.

3.3 The Electrodeposition Process

With the above guidelines for the electrolyte and electrode selection, the electrodeposition was conducted with an electrolyte volume of 25ml. The working electrode and counter electrode was separated by about 4cm. The following variations were conducted and the effect on the morphology and composition was observed:

Variations

- The voltage was varied between 450mV - 700mV
- The effect of stirring the electrolytic bath was observed
- The electrolyte was maintained at room temperature and the deposition was repeated at $57^{O}C$
- Slight variations of the concentrations
- 5 grades of silicon wafers(type I - V) and two grades of ITO were used as the working electrode
- The effect of annealing

At every stage of the experiment, the samples were subjected to only one variation at a time. The films were thoroughly rinsed in distilled water to wash off all traces of the electrolyte at the end of the process. Each time a thin film is deposited, the EDX and XRD tests were done apart from visual observation to study the actual effect of the variation.

The following outcome was observed from the above mentioned variations. The effect of deposition potential variation was studied by the EDX technique and it was found that a deposition potential of 0.67V had a favourable effect on the film composition (discussed in section 3.5.2). The stirring of the electrolytic bath yielded improved deposition current and film uniformity. This can be explained by the fact that stirring eliminates concentration gradients of free ions in the solution for a more uniform distribution. The effect of heating the electrolyte at $57^{O}C$ had a positive influence on the uniformity and adhesion of the deposited CdTe films. The stirring effect also assists in maintaining the uniformity of the temperature distribution in the electrolyte. Therefore this heating temperature and solution stirring was maintained for all consequent electrodeposition of films.

The concentration variation of the component aqueous solution, which are $CdSO_4$ and TeO_2, in the electrolyte was made in very small proportions. Since the effect observed in the EDX quantitative did not yield any appreciable change in the composition, the earlier mentioned concentrations as described in section 3.2.1 were maintained. The

effect of annealing the CdTe thin films was observed and discussed more closely in the XRD discussions in section 3.5.1. A large amount of experimentation was done on the five different wafer grades namely type I-V. The main differences observed during electrodeposition of these wafers were the rate of deposition and deposition current. However, since type V wafers has a resistivity in the theoretically suitable range of 5-100Ω for optimum photovoltaic conversion, it was most frequently used in most of the depositions as well as for the sputtering procedure. The trend of the deposition current was observed to follow that of the resistivity, where the lower the resistivity the higher the deposition current and hence a higher deposition rate.

3.4 Electron Beam Sputtering - CdTe

CdTe films were also fabricated by electron beam sputtering to compare the physical characteristics and the subsequent solar cell performance. The other purpose is also to obtain first hand experience on the practical aspect of preparing films by this high temperature method.

The substrates used for depositing the film were type V silicon wafer pieces (2cm x 3cm), glass slides (2cm x 3cm) and high conductivity ITO (1cm x 1.5cm). The silicon wafers were cleaned by the prescribed method in chapter 2 and the ITO and glass slides were cleaned as per the electrodeposition requirement. These substrates were mounted in sets of three (silicon, ITO, glass) at four different locations on an aluminium plate and placed face down above the shutter and sputtering source. The sets of substrates were placed at unequal distances from the centre as it was found earlier at the trial stage that the thickness of the film is a factor of its location and distance from the source. Therefore in total, four different sample thickness can be obtained from each sputtering procedure.

Analar grade CdTe granules (99.99% purity) were used as the starting material. These granules were placed in a carbon hearth and raised into position just below the tungsten filament. The bell jar chamber was then replaced and the system was allowed to pump

down to pressure of about 2×10^{-5} mbar in the high vacuum range. Before deposition, degassing of the filament is first done, on the low tension mode. The power is increased to approximately 60% and the vacuum level falls before stabilising once again.

Following degassing, the high tension is applied gradually until a plasma glow is observed. The shutter was then opened for the deposition to take place for about thirty seconds.

3.5 Material Characterisation

The thin films obtained by the prescribed electrodeposition and sputtering methods above were subjected to material characterisation studies as outlined below:

3.5.1 X-ray Diffractometry

The purpose of conducting the X-ray diffraction studies is to ascertain the integrity of the material formed and hence to positively identify the coatings. The presence of the phase of the material or materials present is signified by the peaks present.

The table below shows the theoretical peak values [68, 69, 70] for the cubic and hexagonal CdTe phases, as well as the peaks observed from the electrodeposited and sputtered samples in Figure 3.4, 3.5 and 3.6 from the 2θ angular range of 20° - 50°. The values in the columns indicate the peak angle, the plane orientation and relative intensities.

Table 3.3: Theoretical and Experimental Values of XRD Peaks

Cubic CdTe (Theoretical) ($2\theta^0$)			Hexagonal CdTe (Theoretical) ($2\theta^0$)			Sputtered CdTe (From Figure 3.4 & 3.5)			Electrodeposition CdTe (From Figure 3.6)		
23.68	(111)	100%	23.2	(110)	75%	23.9	(111)	100%	23	(111)	100%
39.47	(220)	15%	24.3	(002)	100%	40	(220)	11%			
46.32	(311)	10%	26.2	(100)	80%						
			40.2	(110)	5%						
			42.4	(103)	3%						
			49.7	(201)	5%						

The generally low intensities are due to the thin nature of the films prepared and it is thus difficult to distinguish the low intensity peaks from the background and it appears diminished. The high intensity peaks however quite apparent. By comparing the relative intensities of the peaks observed with theoretical values of the cubic and hexagonal phases, it is apparently more likely that CdTe films produced experimentally exists in the cubic phase. This is because some associated high intensity peaks of the hexagonal phase at the angular values 23.2^0 and 26.2^0 are not present.

It can therefore be deduced based on the diffraction data that the films formed by sputtering and electrodeposition are of the cubic CdTe phase. This deduction is in close relation to work published elsewhere [64] whereby films prepared by the similar technique as presented in this work yielded CdTe films of the cubic phase.

Figure 3.4 shows the diffractogram of a thin (3.4a, ≈400nm) and thick (3.4c, ≈800nm) film of CdTe which was sputtered on silicon. The main features of the peaks remain the same but the thicker film displays a higher intensity CdTe peak, which can be attributed to the growth of the material incorporated into the diffraction process. Figure 3.4b and 3.4d show the diffractogram obtained when the samples 3.4a and 3.4b were annealed for one hour in vacuum at 473K. Once again an increase in the intensity is observed with no change in features. This can be explained by the fact that annealing actually increases the grain size and promotes the change of the metastable phases to a more stable cubic phase [70]

Figure 3.5 shows the diffractograms of CdTe sputtered on glass. Once again 3.5a and 3.5c represent thin (≈ 400nm) and thick (≈ 800nm) samples of CdTe and 3.5b and 3.5d are the diffractogram of these samples annealed at 473K for one hour in vacuum. The explanations behind the increase in intensity remain the same as when sputtered on silicon. This conclusively proves that the behaviour of the film is not dependant on the substrate type whether it being amorphous as in glass or highly crystalline as in the silicon substrate.

Figure 3.4 : XRD of CdTe Sputtered on Silicon

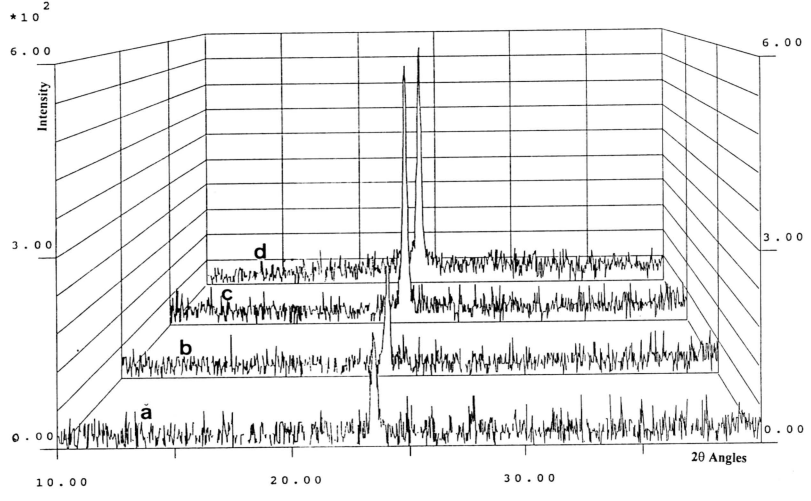

a: Thin Film, b: Thin Film Annealed, c Thick Film, d: Thick Film Annealed

Figure 3.5 : XRD of CdTe Sputtered on Glass

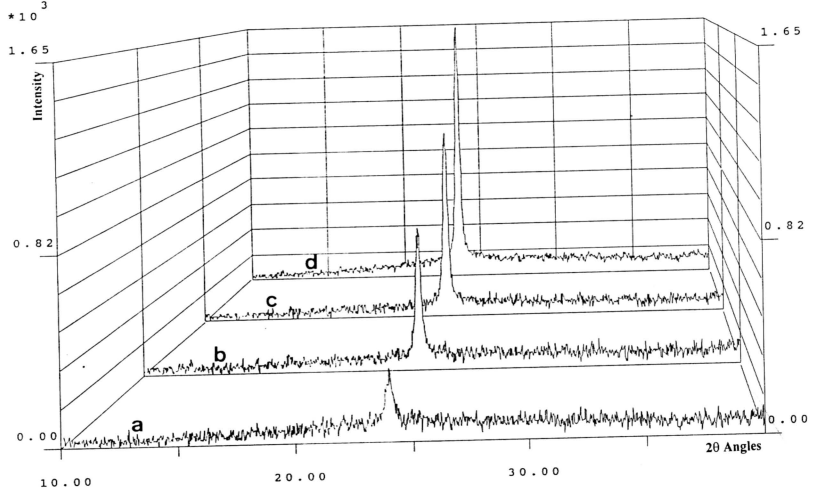

a: Thin Film, b: Thin Film Annealed, c Thick Film, d: Thick Film Annealed

Figure 3.6 : XRD of CdTe Electrodeposited on Silicon and ITO

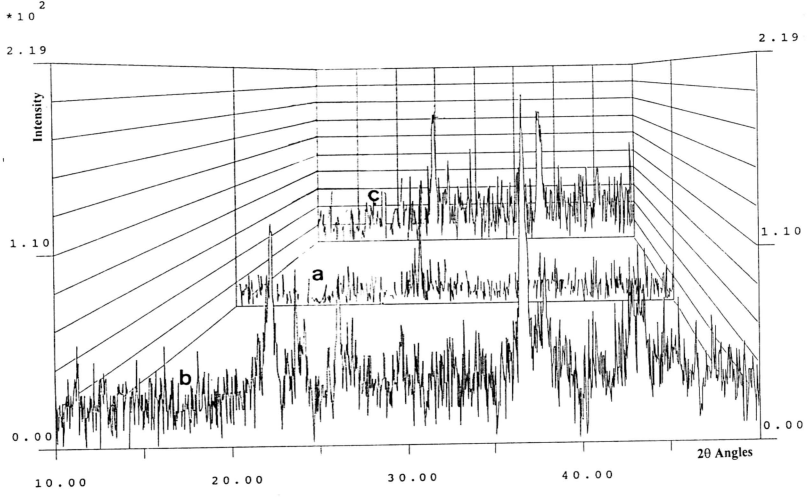

a: Thin Film on Si (0.45V), b: Thin Film on Si (0.67V), c: Thin Film on ITO (0.67V)

Figure 3.6 shows the diffractogram of samples electrodeposited on silicon (3.6a and 3.6b) and on indium tin oxide (ITO) (3.6c). The film on 3.6a was electrodeposited at 0.45V and 3.6b at 0.67V. Both diffractograms show a basic difference in the number of peaks corresponding to the cubic CdTe phase. Figure 3.6a has only one major peak (23°), whereas 3.6b has 2 major peaks (23° and 37°) that corresponded to cubic CdTe. We once again deduce that the films are not of the hexagonal phase due to the absence of two high intensity peaks at 23.2^0 and 26.2^0. This enables us to identify a more suitable voltage which also agrees with what was prescribed by past literature [64] of 0.67V to obtain a more crystalline film which would result in better solar efficiency. Diffractogram 3.6c shows similar features to that of 3.6b indicating that a similar film formation is obtained by electrodeposition on ITO glass. These films deposited on transparent ITO also assists in obtaining information on the optical characteristics.

3.5.2 Energy Dispersive Analysis of X-rays (EDX)

The quantitative analysis was done by the energy dispersive analysis of X-rays (EDX) technique. This method is highly convenient as it is coupled to the SEM and it is possible to view the exact area where the quantification is being done. It is also not necessary to form calibration curves for individual elements as the EDX has a built in mathematical algorithm to compensate for atomic number (Z), absorption (A) and fluorescence (F) effects from individual elements in individual samples. For the purpose of consistency and best averaging of the quantification, the electron beam was scanned over the largest possible surface of the CdTe thin film by selecting the lowest magnification mode possible in the SEM.

The EDX technique was vital in the early stages to ascertain the effect of deposition voltage and deposition time on the composition of the film. It is of course impractical to present all the acquired data and six of the most significant will be shown as figure 3.7(a-c) and 3.8(a-c) here.

Figure 3.7a shows the EDX spectra of CdTe deposited on silicon at a voltage of 0.45V, Figure 3.7b at 0.67V and 3.7c at 0.8V. The effect of the deposition voltage on the percentage of cadmium and tellurium is shown in table 3.4 below.

Table 3.4: The Effect of Deposition Voltage on the Composition of CdTe

Figure	Deposition Voltage (V)	Cadmium (Cd%)	Tellurium (Te%)
3.7a	0.45	38.41	61.59
3.7b	0.67	52	48
3.7c	0.85	70.92	29.08

From the EDX spectra and the quantification spectra, it can be clearly seen that cadmium and tellurium form closest to the CdTe 1:1 ratio when the deposition voltage of 0.67V is applied. With this ascertation, all subsequent films were deposited at this particular voltage and used for further characterisation and PV cell performance analysis. At a voltage of 0.45V, the films were found to be tellurium rich. This is in close relation with theoretical predictions from the voltammogram.

Figure 3.8a - 3.8c show the EDX spectra of CdTe deposited on silicon for a range of deposition times at 0.67V. Figure 3.8a is the spectra for a CdTe film deposited for ten minutes with a change of the copper counter electrode after five minutes. Figure 3.8b and 3.8c are the respective spectra of samples coated for thirty minutes and one hour. The comparative thickness is observed and can be predicted by the intensities of the cadmium, tellurium and silicon peaks. Since CdTe is coated on silicon, the silicon peak appears subdued as the films are thick and the electron beam is unable to penetrate the films to generate its characteristic silicon X-rays. The relative intensities of the silicon peaks helps us deduce the comparative thickness of the films. The quantification is fully computerised and is based on the integration of the peak area and not peak height. We can therefore observe that the quantification is not in proportion to the peak height in most cases. The obtained quantification data and observations are tabulated below.

Table 3.5 : The Effect of Deposition Time on Film Thickness and Composition

Figure	Deposition Time (minutes)	Comparative Thickness	Cadmium (Cd%)	Tellurium (Te%)
3.8a	10	Thin	47.77	52.23
3.8b	30	Medium	41.61	58.59
3.8c	60	Thick	43.42	56.58
3.8d	Sputtered	Medium	58.24	41.76

For spectra 3.8a, it was noted that no copper peaks were observed. But for 3.8b and 3.8c, increasing amount of copper had diffused into the films. The changes observed in the cadmium and tellurium composition in all three spectra gives a close approximation to a 1:1 ratio. A slight variation can be observed in absolute percentages and can be attributed to non uniformity of the film at various analysis locations of the sample and normal errors associated with the technique.

From here, we can conclude that longer deposition times does not change the CdTe film composition significantly but if we do not change the copper counter electrode or deposit for longer periods of time, it could cause the diffusion of copper into the deposited film. The presence of the highly conducting copper could be detrimental to the eventual PV cell coating as it could prove to be an electronic trap and reduce electron mobility. Thick films would also have a detrimental effect on the PV cell performance due to the inability of light to illuminate the formed p-n junction and also because of absorption losses. Thick films also increase the overall cell resistance. Overall, the EDX quantification had conclusively helped in ascertaining the optimum deposition voltage and time for the electrodeposition of CdTe thin films.

Figure 3.8d shows the EDX spectra of sputtered CdTe. It can be seen that an almost 1:1 stoichiometry of Cd : Te is formed. This is an expected outcome as the starting material used in the sputtering process were pure CdTe granules.

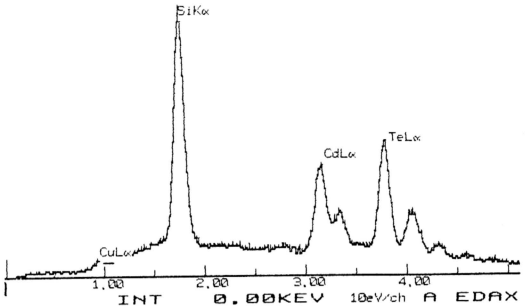

Figure 3.7a : EDX Spectra for CdTe Electrodeposited on Si at 0.45V

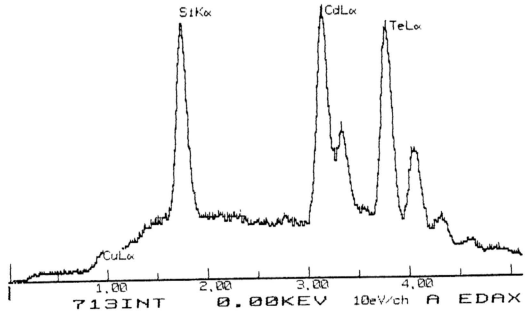

Figure 3.7b : EDX Spectra for CdTe Electrodeposited on Si at 0.67V

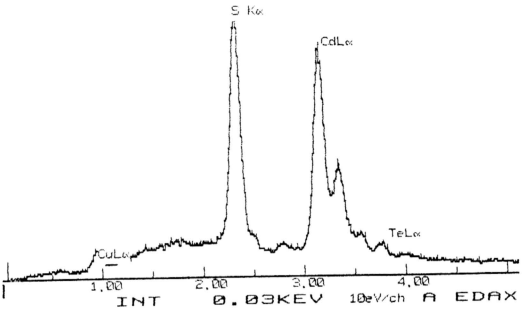

Figure 3.7c : EDX Spectra for CdTe Electrodeposited on Si at 0.8V

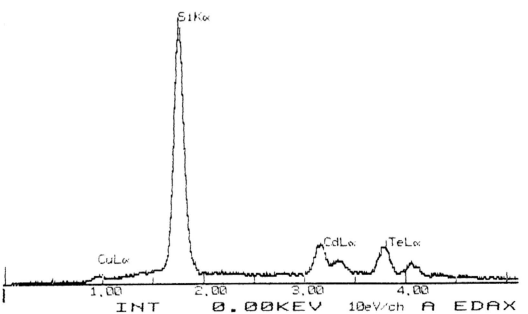

Figure 3.8a : EDX Spectra for CdTe Electrodeposited on Si for 10 minutes (at o.67V)

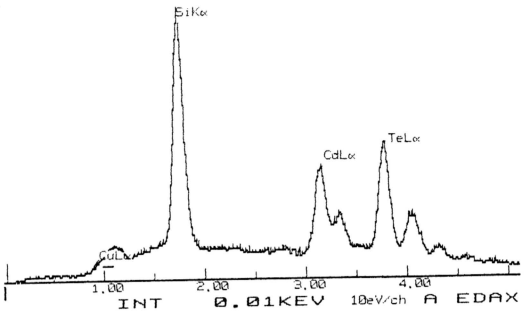

Figure 3.8b : EDX Spectra for CdTe Electrodeposited on Si for 30 minutes (at o.67V)

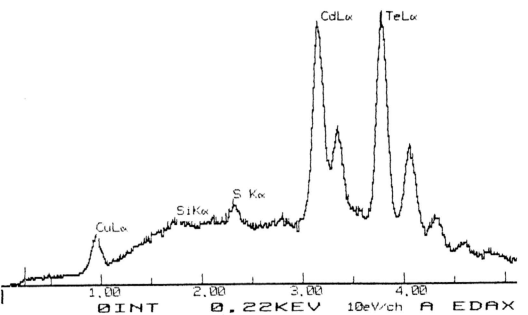

Figure 3.8c : EDX Spectra for CdTe Electrodeposited on Si for 60 minutes (at o.67V)

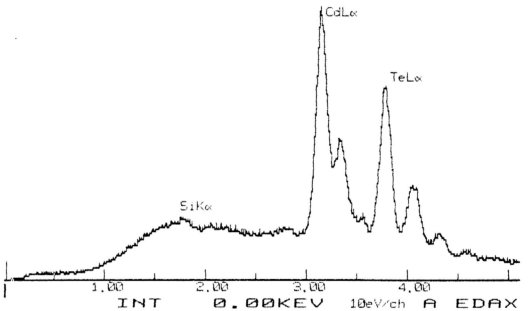

Figure 3.8d : EDX Spectra for CdTe Sputtered on Si

3.5.3 Scanning Electron Microscopy (SEM)

The purpose of conducting studies by the scanning electron microscopy technique is to determine the surface morphology and structures of thin films [71] coated by the sputtering technique and electrodeposition (on Silicon and ITO). The micrographs obtained which revealed structural features were obtained in magnifications ranging from 5000X to 30000X. The quality and the significance of the micrograph was studied and the relevant features at specific magnifications were observed. On this basis, several of the micrographs were selected for discussion here.

Figures 3.9a and 3.9b show the micrographs of CdTe sputtered on Silicon at 10000X and 17000X magnification. It is apparent that a film of a very uniform polycrystalline nature, low porosity and with fine grains is formed. From the micrograph at 15000X magnification, the average grain size was estimated to be 0.1 - 0.3μm. Higher magnification micrographs at 30000X did not yield further information as the resolution was insufficient to determine the grain boundaries.

The micrographs of CdTe films electrodeposited on Silicon are shown in figures 3.10a, 3.10b and 3.10c at magnifications of 220X, 10000X and 20000X respectively. The low magnification micrograph was produced to show the unique pattern of the surface of an electrodeposited sample. A general polycrystalline pattern can be observed as the surface structure for all the electrodeposited samples in this research (inclusive of CdSe, $CdTe_xSe_{1-x}$) regardless of the substrate. The micrograph at 10000X magnification also shows a porous polycrystalline distribution of particles which is a common feature in electrodeposited samples [ref]. The difference on contrast of the surface particles (light contrast) and the bulk (dark contrast) shows the porosity of the surface. The estimated average particle size is found to be approximately 0.2 - 0.4μm from the 15000X magnification micrograph.

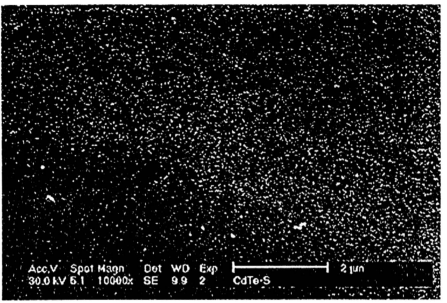

Figure 3.9a : Micrograph of CdTe Thin Film Sputtered on Silicon (10000X)

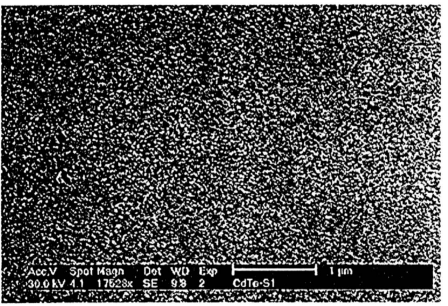

Figure 3.9b : Micrograph of CdTe Thin Film Sputtered on Silicon (17531X)

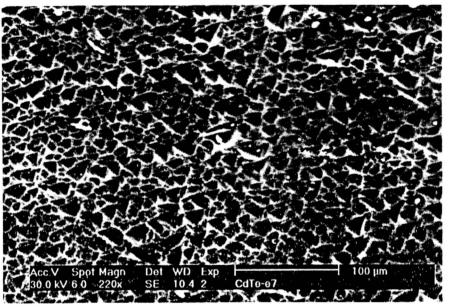

Figure 3.10a : Micrograph of CdTe Thin Film Electrodeposited on Silicon (220X)

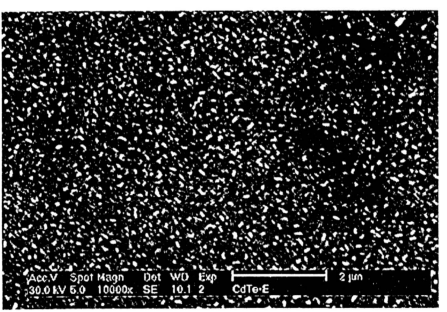

Figure 3.10b : Micrograph of CdTe Thin Film Electrodeposited on Silicon (10000X)

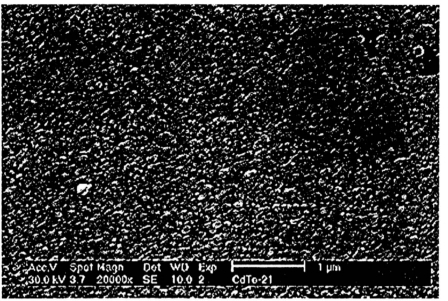

Figure 3.10c : Micrograph of CdTe Thin Film Electrodeposited on Silicon (20000X)

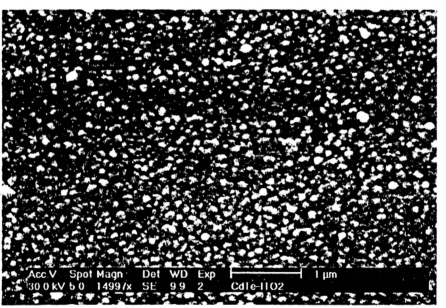

Figure 3.11 : Micrograph of CdTe Thin Film Electrodeposited on ITO (14997X)

A micrograph of CdTe electrodeposited on ITO is shown in figure 3.11. The porous nature can once again be observed from the image contrast and particle size distribution. The average particle size is estimated to be 0.2 - 0.4μm with a uniform distribution without significant dislocations.

3.5.4 Ultraviolet and Visible (UV/VIS) Optical Characterisation

In the transmission spectrum of the UV/VIS region for CdTe electrodeposited on ITO and sputtered on glass, shown in figure 3.12, an interference fringe pattern was observed. This occurrence of transmission fringes is due to the atomic transitions between discrete energy bands and helps deduce the refractive index of the film, the absorption coefficient and the thickness of the film coated on a glass substrate. References were made to published matter [72-78] on the formulas and techniques involved for optical analysis.

From the spectrum, the following data is extracted:

i. λ_1 and λ_2 , that are peaks of two selected fringes that are consecutive

ii. $T_{\lambda 1}$ max, $T_{\lambda 1}$ min, $T_{\lambda 2}$ max and $T_{\lambda 2}$ min, which are the maximum and minimum transmission values at the two selected wavelengths. The refractive index of the thin film is given by :

$$n(\lambda) = [\, N + (N^2 - n_0^2 n_1^2)^{1/2} \,]^{1/2}$$

$$\text{where } N = \frac{n_0^2 + n_1^2}{2} + 2n_0 n_1 \cdot \frac{T_{max} - T_{min}}{T_{max} \cdot T_{min}}$$

n is explicitly determined from T_{max}, T_{min}, n_1, and n_0 at a particular wavelength. n_1 and n_0 is the refractive index of glass and air respectively. Knowing n, we can determine the absorption coefficient α from :

$$\alpha = \frac{\ln A}{t}$$

where: $A = \frac{C_1 [1 - (T_{max}/T_{min})^{1/2}]}{C_2 [1 + (T_{max}/T_{min})^{1/2}]}$

t = film thickness

and $C_1 = (n + n_0)(n_1 + n)$ and $C_2 = (n - n_0)(n_1 - n)$

The film thickness, t, can be calculated from two of the fringes in the spectrum using the equation :

$$t = \frac{M\lambda_1\lambda_2}{2[n(\lambda_1).\lambda_2 - n(\lambda_2).\lambda_1]}$$

where $\lambda_2 > \lambda_1$ and M is the number of oscillations between 2 extremes. This calculation procedure is repeated for numerous consecutive transmission fringes for a larger data population to reduce the effect of instrument and analysis errors that could influence the data.

It is important to note that the number of transmission fringes that occur have a direct relationship with the thickness of the film. The thicker the sample, the greater the number of interference fringes. Figure 3.12 shows the transmission fringes of six samples, three electrodeposited on ITO and three sputtered on glass, that were prepared. The trend of thicker samples having more interference fringes can be observed here. The thinner samples hardly display any fringes and could be said to have only a singular line in some cases.

Using the above mentioned envelope method, the refractive index, the absorption coefficient and the thickness was calculated. The calculations can only be done where the occurrence of multiple fringes were observed. The first step is to fit the curve as shown in one example in figure 3.13 and deduce the values of λ_1, λ_2, $T_{\lambda 1\ max}$, $T_{\lambda 1\ min}$, $T_{\lambda 2\ max}$ and $T_{\lambda 2\ min}$ for two consecutive wavelengths. From these numbers we can

compute the refractive index, thickness and the absorption coefficient, α, of a particular film. An extension of this procedure is to plot a graph of $(\alpha hf)^2$ versus energy. An extrapolation of the absorption edge of this curve to the energy axis would yield the energy gap for the particular coating. This is shown in Figure 3.14. A software program was written in the EXCEL database spreadsheet format to compute all the mentioned values of α, n and t. It was also possible to convert values of A into α and automatically plot the $(\alpha hf)^2$ versus energy graph when sufficient points were obtained.

For the thinner film samples coated for solar cell studies, the lack of transmission fringes does not allow the 'envelope' method to be used. In these cases, the absorption spectra is used for the approximation of the energy gap. The absorption spectra for the same six samples is shown in Figure 3.15. The trend of the absorption spectra shows various gradients of the curves but all of which can be extrapolated to the 800nm to 900nm range. Figure 3.16 shows how the absorption edge is extrapolated to the wavelength axis and the intercept noted. From the relationship, $E\lambda = hc$, the energy gap Eg is derived. (λ used in this calculation is the intercept). The calculated values and theoretical values are tabulated below in table 3.6 and the correlation can be observed.

Table 3.6: The Theoretical Values and the Calculated Values of Various Optical Parameters

Sample	Theoretical refractive index *	Calculated refractive index *	Theoretical energy gap	Calculated energy gap	Calculated thickness (nm)
CdTe Sputtered - Glass (Thick)	2.67	2.71	1.45 eV	1.50	847
CdTe Sputtered - Glass (Thin)	2.67	-	1.45 eV	-	421
CdTe Electrodeposited - ITO (Thick)	2.67	2.9	1.45 eV	1.54	1098
CdTe Electrodeposited - ITO (Medium)	2.67	2.21	1.45 eV	1.38	641.7
CdTe Electrodeposited - on ITO (Thin)	2.67	-	1.45 eV	-	300 (Approximate)

* Theoretical values obtained from [79]

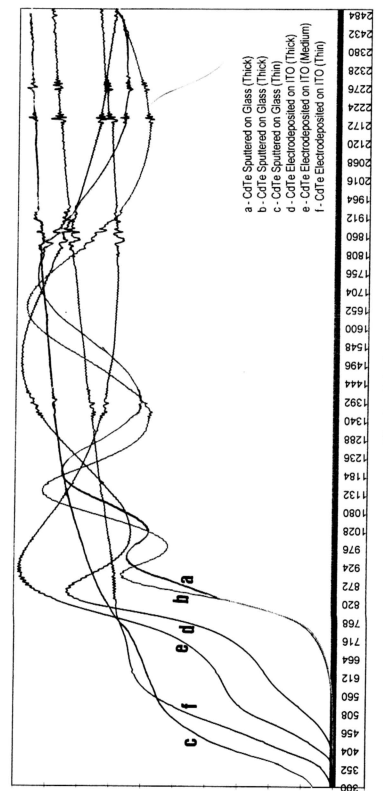

Figure 3.12 : Transmission Spectra (T%) of CdTe Sputtered on Glass and Electrodeposited on ITO

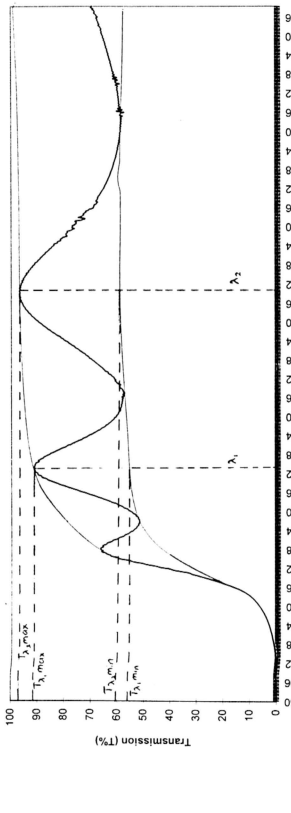

Figure 3.13 : Transmission Spectra of CdTe Sputtered on Glass (Showing fitting for the envelope method)

Figure 3.14 : $(\alpha hf)^2$ vs. Energy - Extrapolated to obtain Energy Gap

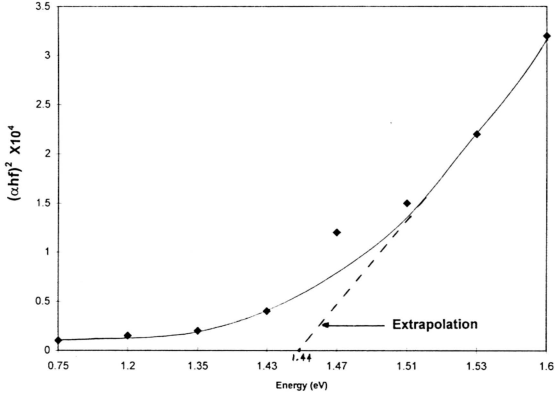

Figure 3.15 : Absorption Spectra of CdTe Sputtered on Glass and Electrodeposited on ITO

Figure 3.16 : Absorption Spectra of CdTe Electrodeposited on ITO

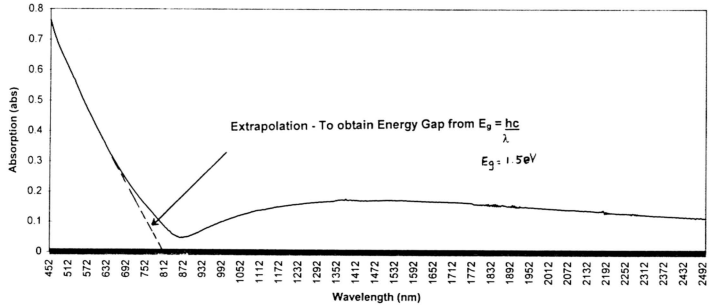

3.6 Electrical Characterisation

3.6.1. Open Circuit Voltage (OCV) and Short Circuit Current (I_{sc})

The electrical characterisation of the obtained films were subjected to two different analysis, namely the open circuit voltage (OCV) and short circuit current (I_{sc}) measurement and the I-V characteristic studies. The OCV and Isc experiments were first conducted on thin CdTe films coated on silicon of various types (type I-V) to determine the suitability of the specific wafer grade in photovoltaic cells. To obtain the open circuit voltage and short circuit current, silver paint is smeared on the film and a fixed area of illumination is masked as described in section 2.5.1. The samples are then illuminated perpendicularly by a 200W tungsten lamp at a distance of 25cm. The results are tabulated below.

Table 3.7: OCV and I_{sc} Characteristics of Five Wafer Grades

Sample	OCV Measured	Resistance (kΩ) Measured	Short Circuit Current, I_{sc} Calculated
Type I	0 mV	110 kΩ	-
Type II	260 mV	135 kΩ	1.93μA
Type III	30 mV	78 kΩ	0.38μA
Type IV	110 mV	90 kΩ	1.22μA
Type V	290 mV	131 kΩ	2.21μA

It was found that the type V wafer yielded the best performance in terms of OCV and Isc. This information was extremely crucial in the initial stages to determine the grade of silicon wafers to be used in further experiments pertaining to cell performance. Type I wafers did not yield any photovoltaic behaviour as the n-CdTe/n-Si interface cannot form a junction which is essential for photovoltaic behaviour. The trend of the cell performance with respect to the resistivity can be seen from this table. Samples with resistivity within the theoretical recommended value of 5-100Ωcm^{-1} (type II and type V) display the best characteristics.

Three samples were selected for the purpose of comparative electrical characterisation studies of the solar cell, which were, a sputtered film of CdTe on silicon type V with a thickness of approximately 421nm (by optical calculations) and thin and thick film of electrodeposited CdTe on silicon type V with a thickness of approximately 600nm and 1100nm respectively. Once again, the silver paint was applied on the surface and the cells illuminated with the relevant electrical contacts established.

Table 3.8: The Comparative OCV and I_{sc} for of Sputtered and Electrodeposited CdTe Films

Sample	OCV Measured	Resistance (kΩ) Measured	Short Circuit Current, I_{sc} Calculated
Sputtered CdTe	295mV	120kΩ	2.45μA
Electrodeposited CdTe (Thin)	290mV	131 kΩ	2.21μA
Electrodeposited CdTe (Thick)	260mV	150 kΩ	1.73μA

The sputtered film produced the highest OCV and I_{sc}. The comparison between the thick and thin electrodeposited films clearly shows that the thick film are detrimental to the overall cell performance due to the lower OCV and I_{sc}. This can be explained by the fact that less of the incident illumination is actually incident on the n-CdTe/p-Si junction due to absorption in the film. The thick film also increases the overall cell resistance and hence reduces the I_{sc}.

3.6.2 Current-Voltage (I-V Characteristic Curve)

The current-voltage (I-V) characteristic curve for the above samples were also done by the method described in section 2.5.2. Figure 3.17 shows the characteristic curve of the same three films as analysed in table 3.8 and an additional ideal curve. The ideal curve is plotted based on estimations of the shunt resistance $R_{SH} \rightarrow \infty$ and series resistance, $R_s = 0$. The influence of series resistance which is largely due to sheet resistance, measurement electrode contacts and substrate resistance is most detrimental in the case of the thick electrodeposited film. The series resistance has a noticeable effect on the I-

V curve, where a reduced generated current seen as a downward shift on the y-axis. The sheet resistance becomes less prominent for the thin electrodeposited CdTe film and the sputtered film.

The effect of shunt resistance is also observed from the I-V curve. The shunt resistance which arises from leakage paths around the p-n junction normally reduces the OCV. The thick film is once again affected most with the effect becoming less prominent for the thinner films. The porous electrodeposited curves have been predicted to be influenced in this way due to the larger grain sizes and higher porosity as compared to the sputtered films.

On the whole, the sputtered films were found to have marginally better I-V characteristics (and hence better power) and this could be most likely due to the lower porosity of the deposition technique. The overall difference is however not very significant and is seen only as a minor shift in the curve. Thus, we can say the CdTe films formed by electrodeposition have a comparable overall performance.

Figure 3.17 : I-V Characteristic Curve of CdTe Sputtered on Si and Electrodeposited on Si